Book Section:
Al-Shammari, AA, Gaffney, EA and Egginton, S orcid.org/0000-0002-3084-9692 (2014) Modelling oxygen capillary supply to striated muscle tissues. In: Ansari, A, (ed.) Advances in Applied Mathematics. Springer Proceedings in Mathematics & Statistics, 87 . Springer International , pp. 13-21. ISBN 9783319069227

https://doi.org/10.1007/978-3-319-06923-4_2

Modelling oxygen capillary supply to striated muscle tissues[¶]

A. A. Al-Shammari[1,2‡], E. A. Gaffney[1] and S. Egginton[3]

[1] *Wolfson Centre for Mathematical Biology, Mathematical Institute, University of Oxford, Oxford OX2 6GG, United Kingdom.*

[2] *Department of Mathematics, Faculty of Sciences, Kuwait University, P.O. Box 5969, Khaldiya 13060, Kuwait.*

[3] *School of Biomedical Sciences, Faculty of Biological Sciences, University of Leeds, Leeds LS2 9JT, United Kingdom.*

[‡] *E-mail: alshammari@maths.ox.ac.uk*

Abstract

The ability to characterise functional capillary supply (FCS) plays a key role in developing effective therapeutic interventions for numerous pathological conditions, such as chronic ischaemia in skeletal or cardiac muscle. Detailed tissue geometry, such as muscle fibre size, has been incorporated into indices of FCS by considering the distribution of Voronoi tessellations ('capillary domains') generated from vessel locations in a plane perpendicular to muscle fibre orientation, implicitly assuming that each Voronoi polygon represents the area of supply of its enclosed capillary. However, to assess the capacity of FCS in muscle we are naturally led to use a modelling framework that can account for the local anatomic and metabolic heterogeneities of muscle fibres. Such a framework can be used to explore the validity of the Voronoi polygon representation of FCS regions while also providing a general platform for robust predictions of FCS.

KEY WORDS: Mathematical modelling, oxygen transport, capillary supply, capillary domains, Voronoi polygons, trapping regions

1. INTRODUCTION

The availability of energy within striated muscle cells (fibres) is essential for sustaining a healthy function. The cellular preference for high energy aerobic metabolism necessitates a continuous supply of oxygen (O_2) for matching the local cellular demand. Such a match is ensured by allowing adequate O_2 delivery from the microcirculation and through a local capillary bed. In particular, capillaries provide the terminal sites for O_2 delivery to and metabolite waste removal from cells, where O_2 diffuses passively across capillary walls and into tissue to meet the local cellular demand (Figs. 1A-1B). Hence a healthy capillary supply is essential for healthy tissue function, thus highlighting the importance of capillary distributions for adequate tissue oxygenation.

Capillary delivery of oxygen is a major limiting factor in the oxygen transport pathway to muscle tissue, especially in the presence of vascular and tissue pathologies. For example, *ischaemia*, a vascular disease involving a restriction in arterial blood supply to tissues (e.g. coronary artery disease), leads to a vascular shortage in oxygen (hypoxemia), which, if left untreated, can further lead to insufficient tissue O_2 supply (hypoxia), complete deprivation of O_2 supply (anoxia), and ultimately necrosis (tissue death). In particular, according to recent estimates from the World Health Organisation, ischaemic heart disease is the leading cause of global human death [14]. While treatment from chronic ischaemia in skeletal and cardiac muscles would certainly benefit from a local enhancement of functional capillary supply (FCS) of oxygen by inducing capillary growth (*angiogenesis*) to match the local tissue demand,

[¶]AA is supported by a studentship from Kuwait University, Kuwait, and by travel grants from the Mathematical Institute and Linacre College, University of Oxford, UK.

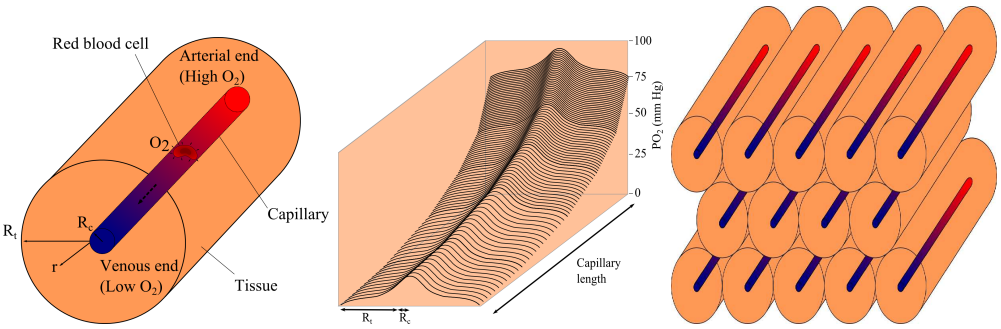

(A) Krogh's cylinder (B) PO_2 profile (C) Cylinder stacking

Figure 1: **A** Traditional view of tissue oxygenation. Estimation of PO_2 within a cylinder of tissue surrounding a capillary of radius R_c; r is the distance from the capillary centre; R_t denotes the cylinder radius where oxygen flux becomes zero [10]. **B** PO_2 at capillary declines monotonically both around and within the fibre; the minimum PO_2 is at the centre of a fibre [5]. **C** Krogh's view of tissue cylinder stacking, where tissue supply voids are inevitable.

we still lack a complete understanding of such interventions. However, even quantifying FCS is fraught with difficulties. While measures of gross capillary supply may highlight a global tissue ischaemia [4], their spatial resolution cannot capture the local tissue pathologies associated with the underlying capillary distribution. At such local resolutions, analyses based on conventional FCS measures can give conflicting results [6], thus potentially leading to poor interpretations of experimental findings.

There has been a growing interest in improving the classification of FCS to tissue and using measures that take into account the local anatomical and metabolic details in experimental studies seeking to assess the extent and location of angiogenesis in striated muscle tissues [3, 5, 15]. Recognising the importance of such attempts, we present a brief account that highlights the modelling developments seeking to quantify the regions of muscle tissue exclusively supplied by individual capillaries as a basis for analyzing FCS.

2. THEORY

2.1. Krogh Cylinder

The idea of quantifying capillary supply by assigning a region of tissue to each capillary was initially conceived by August Krogh in 1919 [10], and subsequently led to his Nobel Prize in physiology. Essentially a *capillary supply region* was defined as the extent of tissue volume diffusively supplied by a capillary. Based on anatomical observations, each capillary was assumed to concentrically supply a hexagonal cylinder. This was further conveniently reduced to an annular cylinder (Krogh Cylinder) with a predefined radius (Fig. 1A), thus leading to a 3D arrangement where capillaries parallel to skeletal muscle fibre axes are symmetrically distributed with their Krogh cylinders stacked evenly (Fig. 1C), inevitably giving rise to tissue supply voids. Along with other simplifications [11], these led to a simple 1D steady-state diffusion problem for oxygen tension, p, with the solution (Krogh-Erland Equation)

$$p(r) \quad = \quad p(R_c) - \frac{M_0 R_t^2}{4D}\left[\log\frac{r^2}{R_c^2} - (r^2 - R_c^2)\right],$$

where R_t and R_c are the tissue and capillary radii with $R_c \leq r \leq R_t$, D is the O_2 diffusion coefficient in tissue, and M_0 is a constant tissue demand for O_2. Combining experimental measurements and geometrical observations of the microvasculature with this formula has led to estimates of the minimum tissue oxygen tension and capillary density [7, 10].

2.2. Capillary Domains

Krogh's attempt to close pack tissue cylinders has led to tissue voids where diffusive supply was geometrically excluded. Gonzalez-Fernandez and Atta [7] addressed this by reformulating

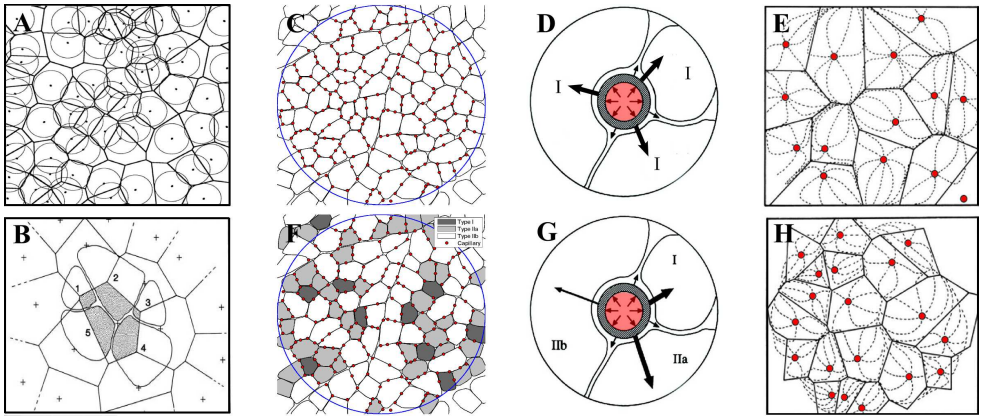

Figure 2: **A** Digitised rat EDL muscle section showing capillary locations (black dots), capillary domains (DOM; polygons), and Krogh cylinders (circles). **B** Fibres partition capillary supply unambiguously by overlapping DOM. **C-D** Uniform muscles have only one type of muscle fibre (e.g. Type I) with spatially homogeneous tissue oxygen demand (MO_2). **E** If capillaries (red disks) have identical transport capacity, the predicted O_2 flux lines (dotted lines) coalesce at the no-flux points that match DOM boundaries (solid lines). **F** Mixed muscles have at least 3 distinct fibre types (types I, IIa, and IIb) with distinct MO_2. **G** O_2 diffusion depends on the local extraction pressures established by differences in MO_2. **H** Given any capillary may be surrounded by distinct fibres, the heterogeneity in fibre composition and MO_2 reduces the fit between no-flux and DOM boundaries for mixed muscles. Our model geometry is obtained by considering a muscle tissue cross section (Figs. **C** & **F**). The tissue region excluding capillaries is denoted by Ω with an external boundary $\partial\Omega$. Capillaries, Ω_i, are treated as circular inclusions within the tissue with a boundary $\partial\Omega_i$ and a uniform radius. Data from [2, 5, 9], with permission.

Krogh's original problem to allow for oxygen supply to the entire domain *via* hexagonal, square, and triangular tissue cylinders. This essentially marked the first formal attempt for modelling a capillary supply region as a *capillary domain* (DOM). While the use of such domains had clearly solved the tissue voids problem, it still maintained the assumption that capillary arrangements within tissue is highly symmetrical. In contrast, capillaries in skeletal muscles are often asymmetrically distributed, thus breaking the symmetry of Krogh's cylinders.

Hoofd and colleagues [8] tackled this question by generalising the symmetry in Krogh's geometrical formalism by allowing each capillary to have a distinct edge of symmetry with each of its neighbours (the bisector of the line connecting neighbouring capillaries). Such a construction identified DOM with the Voronoi tessellation [4, 8] of capillary locations in the plane perpendicular to muscle fibre orientation (see polygons in Fig. 2A). Consequently, the tissue cylinders formed by DOM may have distinct geometries (loss of symmetry), indicating that the Krogh-Erlang equation will assume different solutions for geometrically distinct tissue cylinders. In addition, an 'equivalent' Krogh cylinder, whose cross-sectional area is identically set to the average capillary domain, was alternatively used for all capillaries (compare cylinders to polygons in Fig. 2A). However, the large voids and overlaps associated with these cylinders highlight the inadequacy of using Krogh cylinders to represent regions of capillary supply.

As noted previously, within the framework of DOM, capillaries supply the tissue regions nearest to them, thereby generating a complete tessellation of the tissue plane. This, in turn, allows the detailed anatomical geometry to be incorporated into measures of FCS by considering the overlap of DOM with muscle fibres [5], implicitly assuming that DOM represent the diffusive area of supply of the enclosed capillary (Fig. 2B). However, such geometrical constructs are still simplifications to the diffusive supply regions, which may well be affected by spatial heterogeneities of capillaries and oxygen uptake (Figs. 2F-2H).

2.3. Flux Trapping Regions

Hoofd and colleagues [9] assessed the accuracy of DOM by taking capillaries to be O_2 point sources, which in turn led to an analytical expression for O_2 flux. For a capillary distribution

embedded in a striated muscle with spatially uniform oxygen uptake (Figs. 2C-2D), e.g. cardiac muscle, they found that DOM accurately capture the predicted flux lines (Fig. 2E; [5, 9]). However, it was not clear whether this representation will generalise to all striated muscle tissues, especially in the presence of a feedback between capillaries and tissue. For example, asymmetries in the spatial distribution of capillaries and blood oxygen content as well as heterogeneities in intracellular metabolic and diffusive characteristics are expected to affect the flux of oxygen at the prescribed boundaries of DOM (Figs. 2F-H). In addition, a recent mathematical exploration of this problem has led to the conclusion that DOM are inaccurate for capillary supply representation [13], though based on predictions that were heavily influenced by boundary conditions [1]. Hence, this leaves the question of whether DOM are appropriate in physiological settings.

3. MATHEMATICAL MODEL

Here we present a brief description of our recent mathematical modelling framework which was aimed at assessing the capillary domain approximation and generalising it to capture tissue heterogeneities.

Under maximal aerobic capacity, O_2 transport is effectively 2D and governed by Michaelis-Menten O_2 consumption within muscle fibres, free O_2 diffusion, and O_2 facilitated diffusion by myoglobin (a protein carrier). Averaged intravascular dynamics is fed into the model through a Robin boundary condition at the capillary wall.

Striated muscle tissues are composed of two distinct regions: (1) interstitial spaces and (2) muscle fibres. In addition, muscle fibres can have different intracellular composition which leads to further local specialisations giving rise to distinct fibre types (I, IIa, and IIb). Letting Ω denote the tissue domain exclusive of capillaries (Ω_i), with external boundary $\partial\Omega$, we seek to explore the 2D profile of oxygen tension (PO_2) in Ω (Figs. 2C, 2F)

$$-\nabla\cdot\Big[\underbrace{D(x)\nabla(\alpha(x)p)}_{\text{free diffusive flux}}+\underbrace{C^{Mb}(x)D^{Mb}(x)\left(\frac{dS_{Mb}}{dp}\nabla p\right)}_{\text{myoglobin-facilitated flux}}\Big] = \underbrace{M(x,p),}_{\text{Tissue consumption}} \qquad x\in\Omega, \quad (1)$$

$$-n_i\cdot\big[\alpha(x)D(x)\nabla p\big] = k\left(p_{cap}-p\right), \qquad x\in\partial\Omega_i, \quad (2)$$

$$-n_{\text{tissue}}\cdot\big[\alpha(x)D(x)\nabla p\big]\Big|_{\partial\Omega} = 0, \quad (3)$$

$$S_{Mb}(p)=\frac{p}{p+p_{50,Mb}}, \quad M(x,p) = \frac{M_0(x)p}{p+p_c}, \quad (4)$$

where D and α are the molecular diffusivity and solubility of free oxygen, C^{Mb} and D^{Mb} are the bulk myoglobin (Mb) concentration and diffusivity, S_{Mb} is the equilibrium O_2-saturation of Mb, $p_{50,Mb}$ is the tissue oxygen partial pressure at half Mb-saturation, M is the rate of O_2 consumption in muscle tissue, M_0 is the maximal consumption rate ($VO_{2\max}$) of a muscle fibre, and p_c is the tissue PO_2 value which reflects the partial pressure scale where fibre mitochondria are no longer able to extract oxygen at maximal rate. Parameter values are detailed in [1, 2].

4. COMPUTATIONAL SOLUTION

4.1. PO_2, Oxygen Flux, and Trapping Regions

A direct numerical exploration of the oxygen transport problem within tissue cross sections can be pursued *via* image capture, overlaying a mesh which is faithful to the geometry captured from biopsies and refined within regions of complex geometry (see Figs. 3A-C). This allows a numerical solution of our oxygen transport equations, which capture the biophysics of oxygen delivery while accounting for histological detail. However, the complexity at the microvascular level limits the length scales which may be readily explored in this manner, especially for 3-D simulations, or for simulations within a large parameter space.

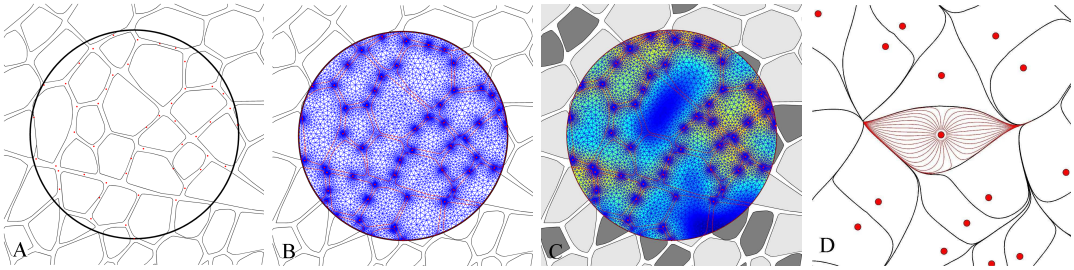

Figure 3: Computational framework. **A** Post-segmentation digitised image of tissue cross section. **B** Finite element mesh generation. **C** Numerical solution to Eqns. 1-4 with fibre-specific parmaters using Matlab's PDE Toolbox [12]. **D** PO_2 flux lines (red) generated for each capillary (disk) by numerically solving $\frac{d\mathbf{x}}{ds} = -\nabla p$ with Trapping Regions delimited (black), where s parameterises he flux lines.

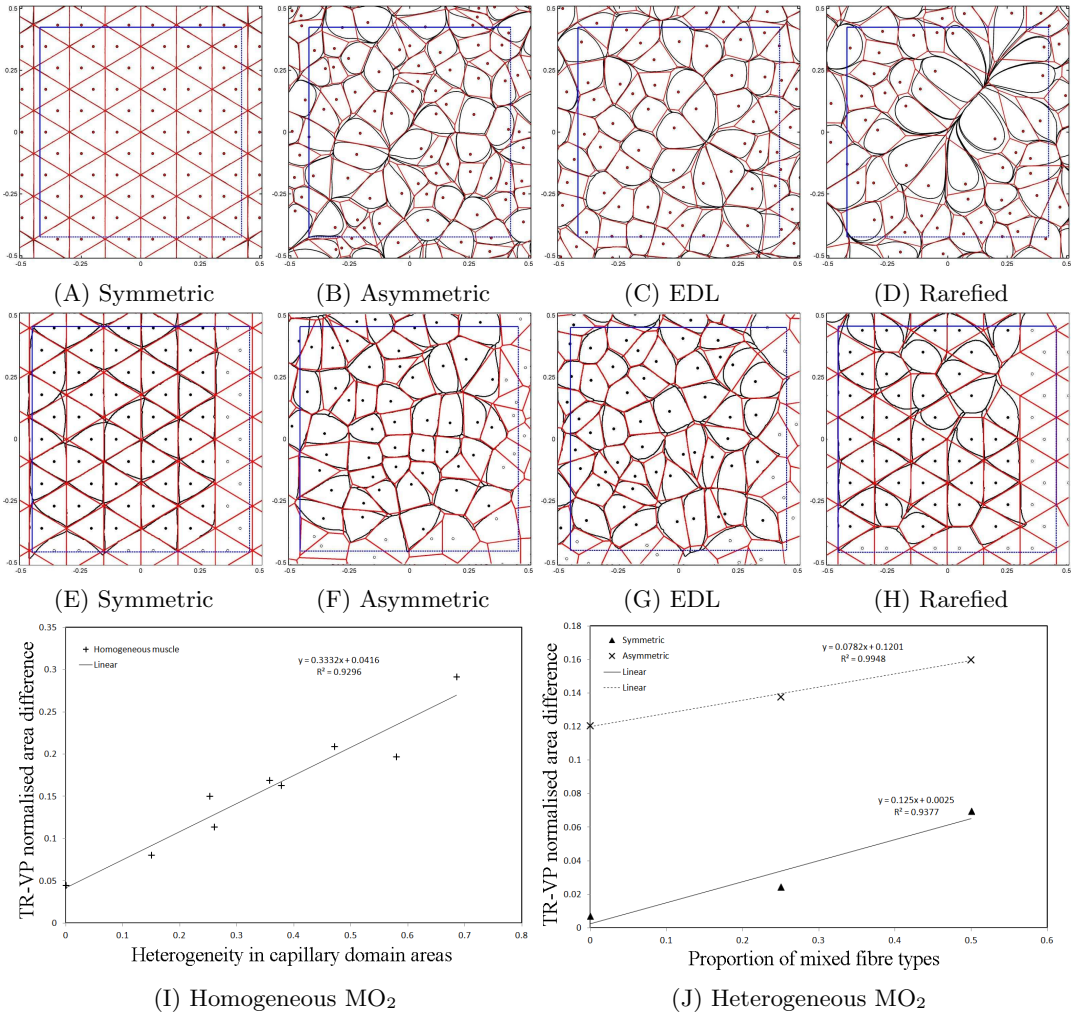

Figure 4: Investigation of the effect of structural and metabolic heterogeneities on the correlation between Capillary Domains (DOM; red) and Trapping Regions (TR; black). Capillary arrangement is *symmetric*, *asymmetric*, from *extensor digitorum longus* muscle, or *rarefied*. Oxygen demand is homogeneous in **A-D** and heterogeneous in **E-H**. Plots of the difference between DOM and TR are given for variation in: (**I**) the spread of DOM areas, and (**J**) the proportion of mixed fibres. Data from [1, 2] with permission.

To determine the supply regions of our model (trapping regions, TR; Fig. 3D), oxygen flux can be first computed by solving the gradient dynamical system, $\frac{dx}{ds} = \nabla p$ where $x(s)$ is a parameterisation of the trapping region boundary, *via* Heun's method. The Hartman-Grobman theorem can then be employed to estimate TR as detailed in [1].

4.2. Capillary Domains vs. Trapping Regions

Using the above framework we can qualitatively and quantitatively assess the area of capillary supply in the presence of heterogeneities (Fig. 4). For example, DOM make a generally accurate approximation of TR (Figs. 4A-4C), with lower accuracy correlating with increased spatial heterogeneities of capillary locations (Fig. 4I). Nonetheless, DOM breakdown in the presence of significant capillary rarefaction (Fig 4D). In addition, increasing the metabolic heterogeneity further accentuates DOM's inaccuracy (Figs. 4E-4H & 4J). In particular, the heterogeneity in capillary arrangements is observed to have a much more pronounced effect on the accuracy of DOM than that of metabolic heterogeneities.

5. DISCUSSION

Voronoi tessellations (capillary domains) may be a useful method for assessing oxygen capillary supply in homogeneous tissue, but their use may be problematic in the presence of extensive capillary rarefaction (functional & structural). Calculation of diffusive oxygen fluxes provides a computationally more intensive alternative. In cases of heterogeneous perfusion, such trapping regions provide a more general representation of capillary supply regions. In addition, this approach will allow incorporation of additional influences of heterogeneity that are absent in the consideration of capillary domains, such as differences in local metabolism or muscle fibre size. Therefore, trapping regions may be used to better inform experimental studies assessing microvascular and tissue dysregulations and pathologies.

REFERENCES

1. A.A. Al-Shammari, E.A. Gaffney and S. Egginton (2012), *Re-evaluating the use of Voronoi Tessellations in the assessment of oxygen supply from capillaries in muscle*, Bulletin of Mathematical Biology, 74(9):2204-31, DOI: 10.1007/s11538-012-9753-x
2. A.A. Al-Shammari, E.A. Gaffney and S. Egginton (2014), *Modelling oxygen capillary supply capacity in mixed muscles: capillary domains revisited*, Journal of Theoretical Biology, *Submitted*.
3. H. Degens, D. Deveci, A. Botto-Van Bemden, L.J.C Hoofd and S. Egginton, S. (2006), *Maintenance of heterogeneity of capillary spacing is essential for adequate oxygenation in the soleus muscle of the growing rat*, Microcirculation, 13:467476.
4. S. Egginton (1990), *Morphometric analysis of tissue capillary supply.* In: Boutilier, RG (ed) Vertebrate Gas Exchange from Environment to Cell. Advances in Comparative and Environmental Physiology 6, 73-141.
5. S. Egginton and H.F. Ross (1992), *Planar analysis of tissue capillary supply*, Society for Experimental Biology Seminar Series , Vol 51: Oxygen Transport in Biological Systems, Cambridge University Press, pp165-195.
6. S. Egginton and E. A. Gaffney (2010), *Tissue capillary supply its quality not quantity that counts!*, Experimental Physiology, 95(10): 971-979.
7. J.M. Gonzalez-Fernandez and S.E. Atta (1972), *Concentration of oxygen around capillaries in polygonal regions of supply*, Mathematical Biosciences, 13:55-69.
8. L. Hoofd, Z. Turek, K. Kubat, B.E.M and S. Kazda (1985), *Variability of intercapillary distance estimated on histological sections of rat heart*, Advances in Experimental Medicine and Biology, 191:239-47.
9. L. Hoofd, Z. Turek and J. Olders (1989), *Calculation of oxygen pressures and fluxes in a flat plane perpendicular to any capillary distribution*, in: "Oxygen Transport to Tissue XI," K. Rakusan, G. Biro, T. K. Goldstick, and Z. Turek, eds., Plenum Press, New York and London, pp. 187-196.
10. A. Krogh (1919), *The number and distribution of capillaries in muscles with calculations of the oxygen pressure head necessary for supplying the tissue*, Journal of Physiology, 52:391-408, 409415, 457-474.
11. F. Kreuzer (1982), *Oxygen supply to tissues: the krogh model and its assumptions*, Experientia, 38:14151426.
12. The Mathworks, Inc. (2013). *Partial Differential Equations Toolbox: User's Guide (R2013b).* Retrieved November 2, 2013 from http://www.mathworks.co.uk/help/pdf_doc/pde/pde.pdf
13. C.Y. Wang and J.B. Bassingthwaitghte (2001), *Capillary supply regions*, Mathematical Biosciences, 173:103114.
14. World Health Organization, *The top 10 causes of death.* Retrieved December 22, 2013 from http://www.who.int/mediacentre/factsheets/fs310/en/
15. R.C.I. Wüst, S.L. Gibbings and H. Degens (2009). *Fiber capillary supply related to fiber size and oxidative capacity in human and rat skeletal muscle*, P. Liss, P. Hansell, D.F. Bruley and D.K. Harrison (eds.), Oxygen Transport to Tissue XXX , vol. 645 of Advances in Experimental Medicine and Biology, pp. 7580.